

# Decalcification of cement paste in $\text{NH}_4\text{NO}_3$ solution: microstructural alterations and its influence on the transport properties

Quoc Tri Phung<sup>1,2</sup>, Norbert Maes<sup>2</sup>, Diederik Jacques<sup>2</sup>, Geert De Schutter<sup>2</sup>, Guang Ye<sup>2,3</sup>

<sup>1</sup> *Magnel Laboratory for Concrete Research,  
Ghent University,  
Technologiepark Zwijnaarde 904, 9052 Ghent, Belgium*

<sup>2</sup> *Institute of Health, Environment and Safety,  
Belgian Nuclear Research Centre (SCK•CEN),  
Boeretang 200, 2400 Mol, Belgium*

<sup>3</sup> *Faculty of Civil Engineering & Geosciences,  
Delft University of Technology,  
P.O. Box 5048, 2600 GA Delft, The Netherlands*

## Abstract

Leaching of cement-based materials changes its properties such as a reduction in pH, an increase in porosity and transport properties and a detrimental effect on properties related to long-term durability. Therefore, a better understanding of leaching process is important including the relevant long-term effects for concretes used in waste disposal systems. However, the decalcification process is not easy to capture because it is extremely slow. In this study, an ammonium nitrate ( $\text{NH}_4\text{NO}_3$ ) solution of 6 mol/l was used to accelerate the leaching kinetics. The experiments were performed on cement paste samples with different water/powder and limestone filler replacement ratios. The change of sample mass over time was monitored, and the amount of calcium ion leached out during the test was determined. Different post-analysis techniques like SEM, MIP and  $\text{N}_2$ -adsorption were used to characterize the microstructural changes, while the degraded front was determined by phenolphthalein spraying. The effect of accelerated leaching on transport properties was studied by measuring the change in water permeability.

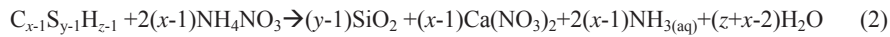
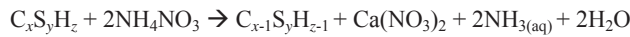
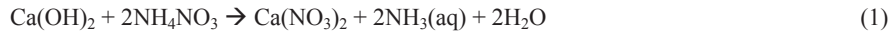
Results show that (i)  $\text{NH}_4\text{NO}_3$  solution is an aggressive but suitable agent to be used to accelerate the Ca leaching in cementitious materials while still keeping the “nature” of leaching; (ii) the square-root-time law of degradation is applicable under accelerated conditions; (iii) the porosity of the leached samples increases significantly and the critical pore size is shifted to larger radius; and (iv) the BET specific surface area of the leached sample is also significantly increased. These changes result in a significant increase in water permeability.

## 1 Introduction

Calcium leaching causes a change in cement mineralogy which results in a pH decrease [1]. This has a detrimental effect on the mechanical properties and may induce rebar corrosion (although corrosion is at higher risk during chloride ingress and atmospheric carbonation) all affecting durability aspect of engineered structures as bridges, dams, water tanks etc. However, calcium leaching is an extremely slow process with a leaching front progression of a few mm in hundreds of years under natural conditions [2]. As such, it is not a critical degradation process for “daily” applications of concrete. However, this is no longer true when we can consider the use of concrete disposal of radioactive waste, in which concrete is used for chemical containment of the waste for very long time. Other properties, such as the chemical environment (contributing to sorption or (co-)precipitation) or flow and transport properties, are of utmost importance.

In order to study the long-term evolution of microstructural and transport properties of concrete during calcium leaching, an accelerated leaching experiment is a relevant approach to better understand the effects caused by the leaching phenomenon on microstructure and transport properties. Acceleration is also a good way to verify prediction models. A variety of accelerated methods have

been proposed applying an electrical field [3], using deionized water [4, 5], using low pH solutions [6, 7] or applying flow- through conditions [8]. One of the most popular methods is leaching under diffusion-controlled conditions with an ammonium nitrate solution as a boundary solution. The  $\text{NH}_4\text{NO}_3$  solution does not only accelerate the leaching process by its low pH, but also because it significantly increases the solubility of leachable phases in the cementitious matrix, mainly portlandite (CH) and the calcium silicate hydrates (C-S-H) as:



Because calcium nitrate is a very soluble salt, the Ca concentration in the pore solution highly increases. Furthermore,  $\text{NH}_3$  escapes from the system which imposes irreversible reactions to the right and continuously prevents the system to reach equilibrium.

Previous studies focused on the prediction of the degraded depth of leached materials via simplified models [9, 10] or the experimental characterization of changes in mechanical behavior [11, 12]. A few studies described microstructural alterations after leaching [10, 11] and the effects of leaching on transport properties [13, 14]. This study aims at establishing relationships between microstructural alterations and permeability changes after leaching of hardened cement paste. This is done by means of imposing an aggressive environment ( $\text{NH}_4\text{NO}_3$ ) to the cement and examining leached samples by quantitative and qualitative analyses. The microstructural characterization was performed using several post-analysis techniques including Scanning Electron Microscopy (SEM), Mercury Intrusion Porosimetry (MIP) and Nitrogen adsorption method (BET). The degraded front was determined by phenolphthalein spraying, while the effect of accelerated leaching on transport properties was studied by measuring changes in water permeability by the method proposed in [15].

## 2 Accelerated leaching experiments

### 2.1 Materials

Experiments were performed on cement pastes with two water/cement ratios of 0.325 (series S1) and 0.425 (series S2). A full characterization was only performed on series S2. Type I ordinary Portland cement (CEM I 52.5 N) was used. The cement has Blaine specific surface of  $4350 \text{ cm}^2/\text{g}$  and density of  $3.10 \text{ g/cm}^3$ . Table 1 gives a summary of the chemical properties. Ammonium nitrate,  $\text{NH}_4\text{NO}_3$ , solution 6 mol/l was used to accelerate the leaching process.

Table 1 Chemical composition and some properties of the cement CEM I 52.5 N (as provided by the manufacturer)

CaO	SiO <sub>2</sub>	Fe <sub>2</sub> O <sub>3</sub>	Al <sub>2</sub> O <sub>3</sub>	Sulphate SO <sub>3</sub>	C <sub>3</sub> A
63.0%	20.0%	3.0%	5.0%	2.9%	7.0%
Chromium(VI)	Cl <sup>-</sup>	Na <sub>2</sub> O eq.	Loss on ignition	Insoluble residue	
<0.0002%	0.06%	0.85%	1.60%	0.50%	

### 2.2 Test setup

Cement paste is poured in a cylindrical PVC tube with inner diameter of 97.5 mm. The sample is then rotated for 24 hours to prevent segregation [15]. Afterwards, the sample is cured in sealed condition in a controlled temperature room ( $22^\circ\text{C} \pm 2^\circ\text{C}$ ) for 27 days. 28-day-cured cement paste is sawed into 25-mm thick slices. In order to study one dimensional leaching (along central axis), the PVC cover remained on the surrounding side of the cement paste slice. Additionally, epoxy resin is poured to fill the gap (if present) between the PVC cover and the cement paste as shown in Fig. 1 (left). In such way radial leaching is prevented.

The cement slices are saturated in saturated lime solution to avoid leaching before starting experiments following the procedure given in [15]. The saturated cement slices are immersed in ammonium nitrate solution chambers with a capacity of 1.2 liters of solution. The ratio between  $\text{NH}_4\text{NO}_3$  solution over the contact surface area of sample is  $8 \text{ cm}^3/\text{cm}^2$ . This factor is chosen to ensure that the pH of solution is always lower than 9.25. When a higher pH values are reached, the solution needs to

be changed to maintain leaching acceleration [16]. The renewal of solution is avoided because the solution is used for Ca quantitative analysis. Fig. 2 shows that the pH evolves during the experiment to stable values of about 9 after a few days.

Nitrogen is injected into the system to prevent carbonation during leaching (Fig. 1, right). The solution is homogenized by a magnetic stirrer. The released nitrogen and ammonia resulting from  $\text{NH}_4\text{NO}_3$  - cement paste reactions escape via a bubbler. There is a sampling line to extract solution for further analysis and follow up the pH of solution. The entire setup consists of 3  $\text{NH}_4\text{NO}_3$  chambers which allow simultaneous execution of three experiments. Reference samples are prepared from the same batch of cement pastes and kept under the same conditions except for immersing in ammonium nitrate solution.

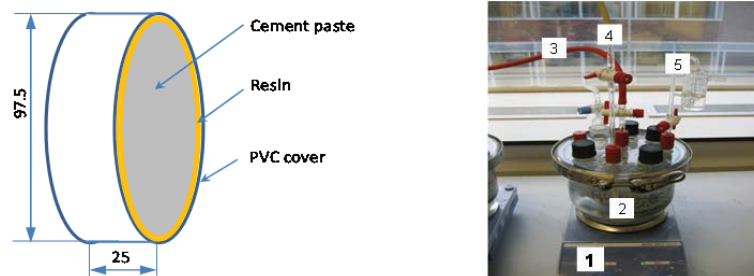


Fig. 1 Preparation of cement paste slice for accelerated leaching in ammonium nitrate 6 mol/l solution (left) and test setup of accelerated leaching using  $\text{NH}_4\text{NO}_3$  solution – 1 - Magnetic stirrer, 2 -  $\text{NH}_4\text{NO}_3$  vessel, 3 - Nitrogen line, 4 - Sampling line, 5 - Bubbler (right)

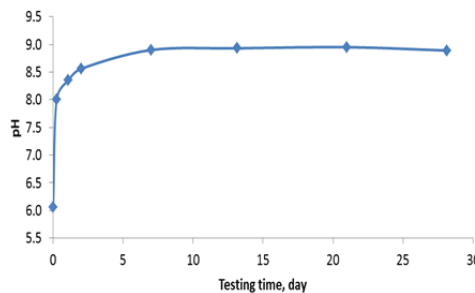


Fig. 2 pH evolution of surrounding solution over testing time – sample w/c = 0.425 (S2)

### 3 Qualitative and quantitative analyses of degraded cement paste

#### 3.1 Degraded depth

The leaching tests are stopped after 7, 14, 21 and 28 days to examine progression of the degraded depth. The leached samples are cut into hemispherical parts and sprayed by a phenolphthalein solution to determine the degraded depth [17]. It is worth noting that exposed surface should be properly cleared after sawing to avoid contamination leading to an incorrect degraded depth measurement. Alternatively, fresh exposed surface can be prepared by axially breaking the sample using a hammer. Note that phenolphthalein indicator only roughly quantifies the leached zone and cannot detect degraded area with pH values of higher than approximately 9.

In order to quantify the amount of calcium leached out from the sample, a sample of the surrounding solution is taken every seven days up to the end of the experiment. The Ca concentration is determined by ion chromatography (IC). Prior to measurement, the solution is filtered through a  $0.45\ \mu\text{m}$  syringe filter, and then diluted 1:1000 with milli-Q water. Measurements are performed on both series S1 and S2.

#### 3.2 Microstructural changes

The changes in microstructure of the leached samples are examined via MIP (overall porosity and pore size distribution - PSD), nitrogen adsorption (BET specific surface area and PSD) and SEM-

EDX (structural information and chemical composition). The measurements are performed on both reference and degraded samples.

Dried samples are required for these techniques. In order to minimize the influence of drying process on the microstructure of the samples, freeze drying is chosen to prepare samples for MIP and nitrogen adsorption measurements. By freeze drying, water crystals sublimate preventing micro cracks generation because of capillary stress generation if drying passes through the liquid state [18]. This method also gives a dried sample in a quite fast period. Samples are directly immersed in liquid nitrogen until the escape of gas bubbles stops. Subsequently, the samples are transferred to a vacuum chamber where a vacuum under  $10^{-2}$  mbar is applied for 24 hours. For SEM measurements, the dried samples are impregnated in a high strength and extremely low viscosity resin before polishing. The polished samples are then coated by a thin gold layer to prevent charging during SEM examination.

MIP experiments are performed on PASCAL 140/440 porosimeter in which the pressure of mercury is continuously increased up to a maximum pressure of 200 MPa. Nitrogen adsorption measurements are done on a TriStar II 3020 Micromeritics. SEM measurements of samples are done using a JEOL JSM 6610 scanning electron microscope. Energy Dispersive X-ray analysis (EDX) is carried out with the aid of ESPRIT Software. All measurements are conducted on leached series S2 samples after 28 day exposure in  $\text{NH}_4\text{NO}_3$  solution.

#### 4 Changes in transport properties

After the leaching tests, the samples of series S2 are stored in tap water until permeability measurements, to prevent drying of the samples and migration of calcium nitro-aluminate (a product of reaction between calcium nitrate and hydrated aluminates) to the surface which can generate micro cracks [19]. Prior to permeability measurements, the samples are embedded in polycarbonate rings by resin under condition of 100 % relative humidity. Water permeability is determined using a controlled constant flow method as proposed in [15]. Measurements are performed on reference and leached samples at different immersed time in  $\text{NH}_4\text{NO}_3$  solutions: 1, 2 and 8 weeks to see the effects of degradation degree on permeability. Care must be taken when measuring permeability of leached samples. Due to the significant decrease in strength of leached samples, the maximum pressure applied on leached samples is limited to 5 bar to prevent mechanically induced cracking and the shrinkage of pore system under compression, while a pressure of above 10 bar can be applied on reference samples to reduce the testing time.

### 5 Results and discussion

#### 5.1 Leached depth and loss of Ca

The degraded depth linearly increases with the square root of immersed time in  $\text{NH}_4\text{NO}_3$  as shown in Fig. 3 (left). This is one of the indicators which illustrates that leaching in ammonium nitrate solution is still a diffusion controlled phenomenon. A rate of  $1.73 \text{ mm/day}^{1/2}$  for the decalcification front propagation of series S2 is found which is quite similar to results reported in [14] despite a slight difference in w/c ratio (0.425 compared to 0.45). Series S1 has a slower degradation rate of  $0.97 \text{ mm/day}^{1/2}$  due to lower w/c ratio.

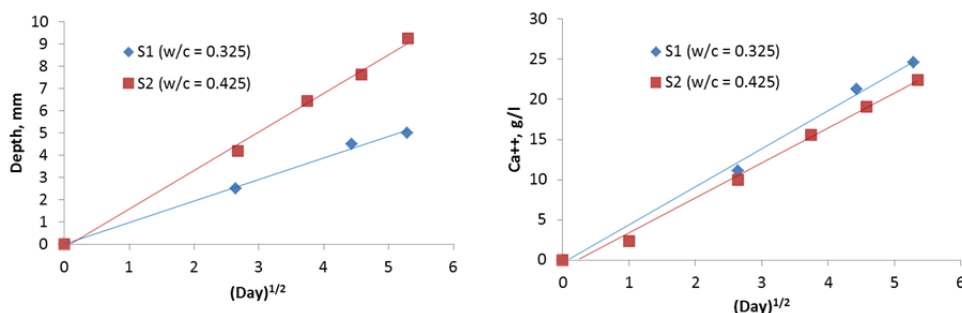


Fig. 3 Degraded depth (left) and amount of leached Ca (right) concentration over immersed duration of time of cement paste in 6 mol/l  $\text{NH}_4\text{NO}_3$

Fig. 3 (right) presents the increase in Ca concentration in surrounding solution which is linearly related to the amount of calcium leached out from cement paste result of leaching. Again, a linear relation of leached Ca concentration as a function of square root of time is shown. It has been seen that series S2 has higher degraded depth compared to series S1. However, the amount of leached calcium of series S2 is slightly lower than one of series S1. This can be attributed to a larger leachable calcium amount in series S1 compared to series S2 because of the lower w/c ratio. Therefore, even with slower degradation rate, the amount of Ca in surrounding solution is still higher for series S1.

## 5.2 Porosity, pore size distribution and specific surface area

As mentioned above, pressure of the porosimeter is increased up to 200 MPa during the MIP intrusion process. However, mercury could not intrude into the leached sample when pressure reaches 143 MPa, while for the reference sample the intruded volume continues increasing until the maximum pressure is reached as shown in Fig. 4 (left). Mercury cannot penetrate into a sample when there are no pores anymore or the remaining pore radii are too narrow. There are two possibilities which can explain this phenomenon: (i) the leached sample is compressed and all pores are clogged at a pressure of 144 MPa or (ii) no gel porosity because the C-S-H phase has completely dissolved. However, BET results are in contradiction with the second possibility (shown later). The complete dissolution of portlandite and partial decalcification of C-S-H can induce a strong loss of elasticity. As a result, the ductility of the leached material will be higher. The deformation at failure of leached samples can increase with a factor of 5 in tension and 2 in uniaxial compression [20]. Obviously, during the mercury intrusion process, the sample is under isotropic compression. Therefore, the deformation must be higher than that reported in [20]. In this study, the sample was checked after finishing MIP test to make sure that it was not broken during the test. No broken sample was seen.

The porosimeter interprets the mercury intruded volume due to sample compression as the occurrence of pores. Thus, we follow a procedure proposed in [21] to account for the deformation of the sample. Fig. 4 (right) presents the intrusion curves of a leached sample before and after correction of the compression effect. It can be seen that the pore volume is compressed by 33% which is too high to be disregarded. The pore size distributions obtained by MIP of the reference and leached samples are shown in Fig. 5 (left). It clearly shows that the critical pore size which is the most frequently occurring pore size in interconnected pores shifts to larger size after leaching. Furthermore, the leached sample shows a bimodal distribution compared to the unimodal distribution of the reference sample. The larger critical pore size of leached samples results in higher transport properties of cement-based materials.

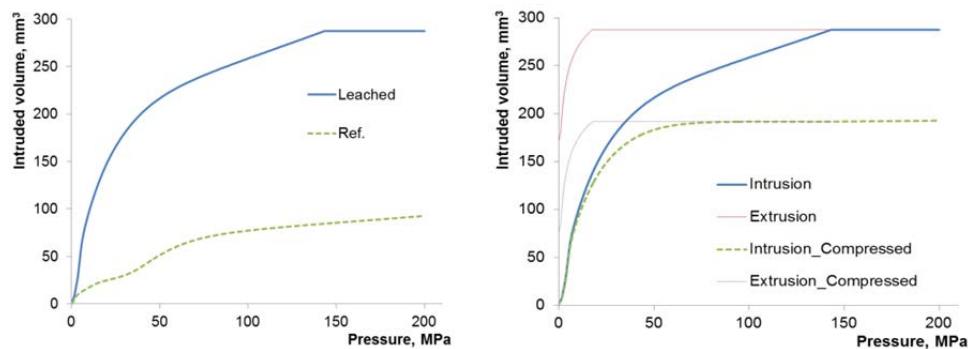


Fig. 4 Intruded volume vs. applied pressure of reference and 28 day-leached samples (left); measurement correction taking into account of compressibility of leached sample (right) of series S2

Even with compression correction, the MIP corrected results cannot be considered as the complete pore distribution of the tested sample because the pore volume of the sample is always higher than the mercury intruded volume due to pore volume compression under pressure. The difference is larger when the pressure increases. In the context of this study, at pressure of approximately 25 MPa (corresponding to a pore diameter of  $0.06 \mu\text{m}$ ), the corrected and uncorrected curves start diverging more and more. For this reason, combining MIP and gas adsorption measurements will give a better understanding of the pore structure of cementitious materials, especially for leached paste. The MIP gives



reasonable results for pore size larger than 0.06  $\mu\text{m}$  while BET provides information on the smaller pores. In this way, pore structure information is obtained in a broad pore size range without the complicating compression effect.

Fig. 5 (right) shows the increase in porosity of the leached sample compared to the reference samples as determined from the combination of MIP and BET methods. In the range of 3 nm - 100  $\mu\text{m}$ , the porosity of leached sample hugely increases up to 38% compared to 15% for the reference sample. Such a large porosity increase is not only due to the decalcification of portlandite but also (partial) C-S-H system because the maximum change in porosity obtained by completely dissolving portlandite is about 12.8% (unpublished modeling result).

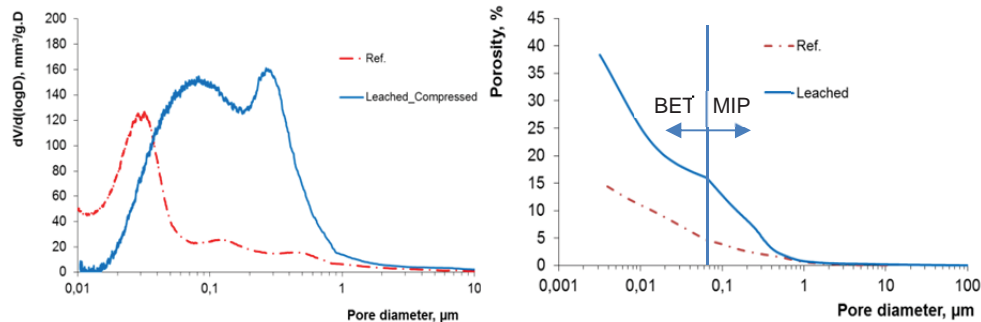


Fig. 5 Influence of calcium leaching on PSD – (left) and increase of porosity due to leaching – series S2 (right)

The surface area determined by BET method of reference and leached samples are 31.6 and 153.6  $\text{m}^2/\text{g}$ , respectively. There is a significant increase in specific surface area of leached material. Such large increase is not only attributed to the dissolution of portlandite but also probably the dissolution of C-S-H. The gel pores of C-S-H which have higher specific surface area compared to micro/meso pores are easier accessible by nitrogen after leaching.

### 5.3 SEM analysis

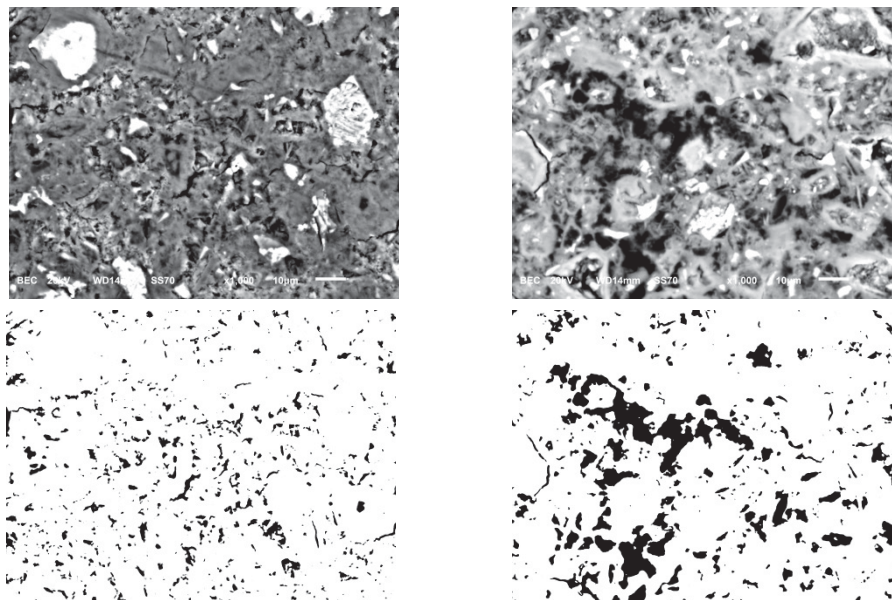


Fig. 6 SEM backscattered electrons images of reference (top-left) and leached (top-right) samples; and porosity (in black) increase due to leaching (bottom) – series S2

Fig. 6 compares the microstructure of a sample with w/c ratio of 0.425 (S2) after 28 day leaching with a reference sample. Leaching clearly increases the pore sizes and total porosity which is in line with the results obtained by MIP and BET. The leaching of Ca and other leachable elements creates connected pathways which can increase the percolation of the pore system and as a result, transport properties can be enhanced. There is an increased connectivity between the pores in the XY direction as observed in at the bottom-right of Fig. 5.

An EDX measurement is performed along a line indicated by the red arrow in Fig 7 (top-left) to quantify the Ca and Si amount. Atomic Ca/Si ratio is converted from normalized mass percentage of Si and Ca and plotted in Fig. 7 (bottom-left). It is found that the average Ca/Si ratio is approximately double in the intact area compared to the degraded area. There is a sudden jump in Ca/Si ratio at distance of about 220  $\mu\text{m}$  because of the fact that it is scanned through Ca-rich region.

Fig. 7 (top-right) shows the spatial distribution of Ca while Fig. 7 (bottom-right) shows the combined spatial distribution of four main elements (Si, Ca, Al and Fe). The intensity of the green color is a measure for the Ca content. The intact area clearly indicates higher amount of Ca. Other elements (Si, Al, Fe) seems to be equally distributed which indicates that those elements do not show significant leaching. Micro cracking is observed in the degraded part in both SEM image (top-left) and mapping figure (bottom-right).

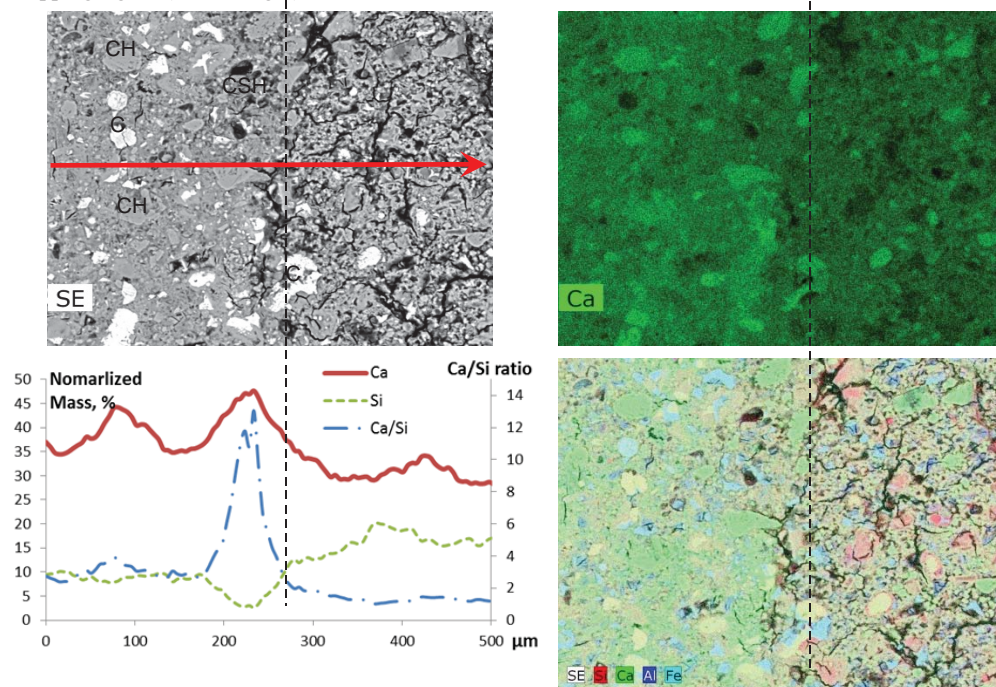


Fig. 7 SEM BE image of transient zone of leached sample: CH = portlandite, CSH = C-S-H phase, C = residual cement clinkers (top-left); Ca/Si ratio along the red arrow (bottom-left); spatial distribution of Ca (right-top) and element (Si, Ca, Al, Fe) mapping generated by x-ray imaging – series S1, field width of 500  $\mu\text{m}$

#### 5.4 Change in permeability

Permeability (expressed here as hydraulic conductivity) is significantly increased after leaching as shown in Table 2. After one week of  $\text{NH}_4\text{NO}_3$  immersion, the hydraulic conductivity increases 6 times, from  $2.3 \times 10^{-13}$  to  $1.4 \times 10^{-12}$  m/s. It continues increasing up to  $3.2 \times 10^{-12}$  m/s and  $1.4 \times 10^{-11}$  m/s after 2 week and 8 week immersion in  $\text{NH}_4\text{NO}_3$ , respectively. It is worth mentioning that the decalcification of the sample is not uniformly with depth and thus, the permeability represents a composite permeability. It is not surprising that permeability increases when degraded depth proceeds further. However, it seems that permeability of the zone with pH larger than 9 also increases. Otherwise it is unlikely that the composite permeability increases so fast – 6 times after 7 day immersion with both sides depth of 8.2 mm over 25mm of sample thickness – because the composite permeability is still

dominated by the permeability of the “non-invasion” zone. Therefore, the authors assume that there exists a relatively thick transition zone in which permeability is increased to a value somewhere between the one of the degraded zone and that of reference sample.

The increase in permeability of degraded material can be explained due to the larger amount of capillary pores (Fig. 4) which is the result of portlandite dissolution. In general, mass transport properties are mainly affected by capillary and large pores [13]. However, because of Ca removal from both portlandite and C-S-H, pathways are created that can increase the connectivity at all pore sizes (micro up to macro). Thus the authors suggest that the dissolution of C-S-H relatively contributes to the change in permeability during leaching. As shown in [22], when a sample in which portlandite is completely dissolved is immersed for 8 days more in a  $\text{NH}_4\text{NO}_3$  solution, the intrinsic permeability slightly increases from  $1.7 \times 10^{-16}$  to  $2.3 \times 10^{-16} \text{ m}^2$ . Which illustrates that decalcification of C-S-H (and probably dissolution of other less leachable phases) can further increase the permeability.

Table 2 Changes in permeability of cement paste with w/c of 0.425 due to leaching in for different immersed periods in 6 mol/l  $\text{NH}_4\text{NO}_3$

Sample	Reference	Leaching period, days		
		7.2	14	57
Permeability, m/s	$2.3 \times 10^{-13}$	$1.4 \times 10^{-12}$	$3.2 \times 10^{-12}$	$1.4 \times 10^{-11}$

## 6 Conclusions

In this study, a  $\text{NH}_4\text{NO}_3$  solution of 6 mol/l was used to accelerate the decalcification of hardened cement paste samples and to examine the effect of decalcification on the microstructural alterations and permeability changes of leached cement-based materials.

The results show that  $\text{NH}_4\text{NO}_3$  solution is an aggressive solution accelerating significantly the leaching kinetics. The square-root-time law of degradation is applicable under accelerated condition indicating diffusive transport conditions. MIP and SEM results confirm a significant increase in porosity of the leached material. A combination of MIP – nitrogen adsorption analysis is needed to obtain information on the pore size distribution changes because the compression effect (due to higher ductility of leached cement paste) is avoided. The accelerated leaching highly alters the microstructure of cement paste to a more porous material which is evidenced by the increase of specific surface area, total porosity and by a coarser pore size. The interconnectivity is increased because of portlandite and partial C-S-H decalcifications. These changes lead to a significant increase in water permeability by one to two orders of magnitude depending on immersed time in  $\text{NH}_4\text{NO}_3$ .

## Acknowledgment

This work is supported by a grant from the Belgium Nuclear Research Centre (SCK•CEN).

## References

- [1] Jacques D, Wang L, Martens E, Mallants D. Modelling chemical degradation of concrete during leaching with rain and soil water types. *Cement and Concrete Research*. 2010;40(8):1306-13.
- [2] Yokozeki K, Watanabe K, Sakata N, Otsuki N. Modeling of leaching from cementitious materials used in underground environment. *Applied Clay Science*. 2004;26(1–4):293-308.
- [3] Saito H, Deguchi A. Leaching tests on different mortars using accelerated electrochemical method. *Cement and Concrete Research*. 2000;30(11):1815-25.
- [4] Haga K, Sutou S, Hironaga M, Tanaka S, Nagasaki S. Effects of porosity on leaching of Ca from hardened ordinary Portland cement paste. *Cement and Concrete Research*. 2005;35(9):1764-75.
- [5] Jain J, Neithalath N. Analysis of calcium leaching behavior of plain and modified cement pastes in pure water. *Cement and Concrete Composites*. 2009;31(3):176-85.



- [6] Bertron A, Duchesne J, Escadeillas G. Accelerated tests of hardened cement pastes alteration by organic acids: analysis of the pH effect. *Cement and Concrete Research*. 2005;35(1):155-66.
- [7] De Windt L, Devillers P. Modeling the degradation of Portland cement pastes by biogenic organic acids. *Cement and Concrete Research*. 2010;40(8):1165-74.
- [8] Butcher EJ, Borwick J, Collier N, Williams SJ. Long term leachate evolution during flow-through leaching of a vault backfill (NRVB). *Mineralogical Magazine*. 2012;76(8):3023-31.
- [9] Wan KS, Li Y, Sun W. Experimental and modelling research of the accelerated calcium leaching of cement paste in ammonium nitrate solution. *Constr Build Mater*. 2013;40:832-46.
- [10] Poyet S, Le Bescop P, Pierre M, Chomat L, Blanc C. Accelerated leaching of cementitious materials using ammonium nitrate (6M): influence of test conditions. *Eur J Environ Civ En*. 2012;16(3-4):336-51.
- [11] Yang H, Jiang L, Zhang Y, Pu Q, Xu Y. Predicting the calcium leaching behavior of cement pastes in aggressive environments. *Constr Build Mater*. 2012;29(0):88-96.
- [12] Nguyen VH, Colina H, Torrenti JM, Boulay C, Nedjar B. Chemo-mechanical coupling behaviour of leached concrete: Part I: Experimental results. *Nucl Eng Des*. 2007;237(20-21):2083-9.
- [13] Perlot C, Verdier J, Carcasses M. Influence of cement type on transport properties and chemical degradation: Application to nuclear waste storage. *Mater Struct*. 2006;39(5):511-23.
- [14] Gallé C, Peycelon H, Bescop PL. Effect of an accelerated chemical degradation on water permeability and pore structure of cementbased materials. *Adv Cem Res*. 2004;16(3):105-14.
- [15] Phung QT, Maes N, De Schutter G, Jacques D, Ye G. Determination of water permeability of cementitious materials using a controlled constant flow method. *Constr Build Mater*. 2013;47(0):1488-96.
- [16] Heukamp FH, Ulm FJ, Germaine JT. Mechanical properties of calcium-leached cement pastes: Triaxial stress states and the influence of the pore pressures. *Cement and Concrete Research*. 2001;31(5):767-74.
- [17] RILEM. CPC-18 Measurement of hardened concrete carbonation depth. *Mater Struct*. 1988;21(6):453-5.
- [18] Gallé C. Effect of drying on cement-based materials pore structure as identified by mercury intrusion porosimetry: A comparative study between oven-, vacuum-, and freeze-drying. *Cement and Concrete Research*. 2001;31(10):1467-77.
- [19] Carde C, Escadeillas G, François AH. Use of ammonium nitrate solution to simulate and accelerate the leaching of cement pastes due to deionized water. *Magazine of Concrete Research*. 1997;49(181):295-301.
- [20] Heukamp F, Ulm F, Germaine J. Does Calcium Leaching Increase Ductility of Cementitious Materials? Evidence from Direct Tensile Tests. *J Mater Civil Eng*. 2005;17(3):307-12.
- [21] Phung QT, Maes N, Jacques D, Schutter GD, Ye G. Microstructural and permeability changes due to accelerated Ca leaching in ammonium nitrate solution. 5th International Conference on Concrete Repair. Belfast, UK. 2014 (submitted).
- [22] Agostini F, Lafhaj Z, Skoczylas F, Loodsveldt H. Experimental study of accelerated leaching on hollow cylinders of mortar. *Cement and Concrete Research*. 2007;37(1):71-8.